O3M SAF FINAL REPORT

Implementation and Verification of a Spike Correction for the SAA

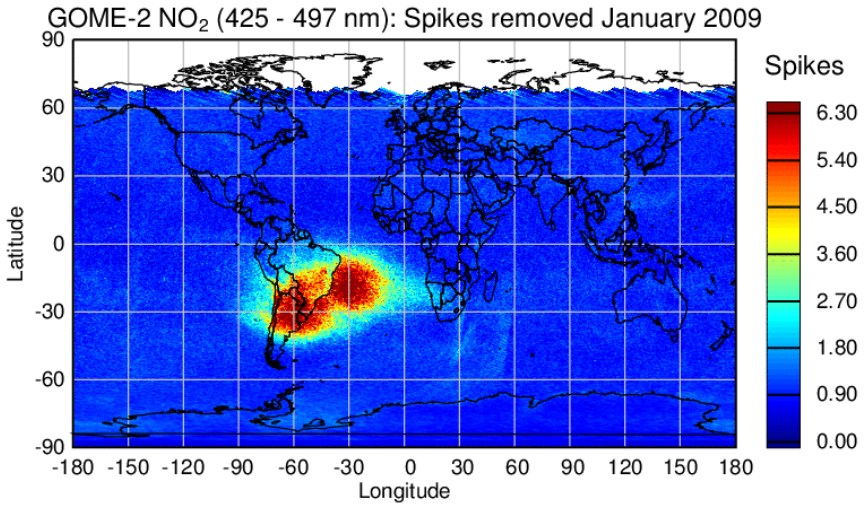

Authors:

Name	Institute
Andreas Richter	**Universität Bremen**
Andreas Hilboll	**Universität Bremen**
Pieter Valks	**German Aerospace Centre**
Diego Loyola	**German Aerospace Centre**

Reporting period: November 2011 – April 2012

Contents

ACRONYMS AND ABBREVIATIONS

AMF	Air Mass Factor
CDOP	Continuous Development and Operations Proposal
DLR	German Aerospace Centre
DOAS	Differential Optical Absorption Spectroscopy
GDP	GOME Data Processor
GOME	Global Ozone Monitoring Experiment
IUP	Institut für Umweltphysik, Universität Bremen
MetOp	Meteorological Operational satellite
NRT	Near-real-time
O3MSAF	Ozone Monitoring Satellite Application Facility
OMI	Ozone Monitoring Instrument
RMS	Root Mean Square
SCIAMACHY	SCanning ImAging spectroMeter for Atmospheric CHartographY
SAA	Southern Atlantic Anomaly
SZA	Solar Zenith Angle

Applicable O3MSAF Documents

[ATBD] Algorithm Theoretical Basis Document for GOME-2 Total Column Products of Ozone, NO2, SO2, BrO, H2O, HCHO, OClO, tropospheric NO2 and Cloud Properties, DLR/GOME-2/ATBD/01, P. Valks, D. Loyola, N. Hao, M. Rix, S. Slijkhuis,.

[PUM] Product User Manual for GOME Total Columns of Ozone, NO2, SO2, BrO, H2O, HCHO, OClO, tropospheric NO2, and Cloud Properties, DLR/GOME/PUM/01, , D. Loyola, W. Zimmer, S. Kiemle, P. Valks, S. Emmadi.

[PRD] Product Requirements Document, SAF/O3M/FMI/RQ/PRD/001/Rev. 06, D. Hovila, J., S. Kiemle, O. Tuinder, H. Joench-Soerensen, F. Karcher, 2008.

INTRODUCTION

The GOME-2 instrument is the operational follow up of the GOME and SCIAMACHY instruments. It flies on the MetOp platforms operated by Eumetsat. The development of operational level 2 trace gas column products for GOME-2 lies in the responsibility of DLR Oberpfaffenhofen, where also the operational GOME and SCIAMACHY data processors are located.

One obvious problem in the GOME-2 data is the strongly increased fitting residuals and scatter of retrieved columns in the region of the Southern Atlantic Anomaly (SAA). While this effect is well known from other instruments such as GOME and SCIAMACHY, the GOME-2 measurements appear to be more affected than others. The origin of the scatter is an anomaly in the Earth's magnetic fields leading to an increased flux of radiation on the satellite instrument which leads to increased noise in the electronics and detector of GOME-2. As a result, radiances measured in the areas affected by the SAA have significantly larger uncertainties, implying also larger uncertainties of the retrieved products. This is illustrated in Figure 1 showing the large scatter of GOME-2 NO_2 columns for individual orbits over South America.

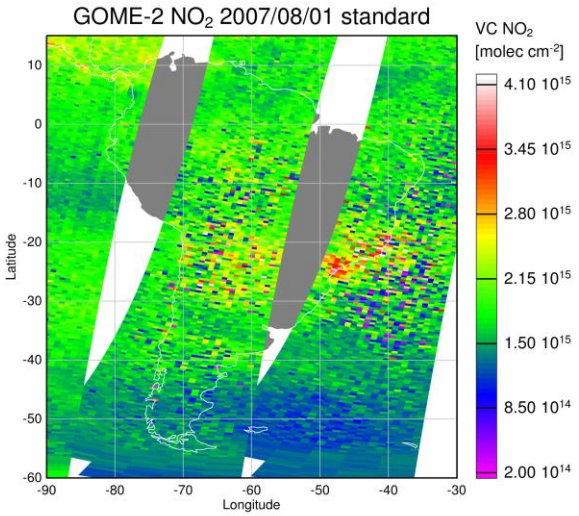

Figure 1: Example of GOME-2 NO_2 fit results over South America illustrating the large scatter of values in the region affected by the SAA

The traditional approach to this problem is to filter data by their chisquare value thus eliminating poor fits. However, over South America, this removes a large fraction of all retrievals even for relatively strong absorbers such as NO_2, and most data for species with smaller absorption such as SO_2 or BrO. It is thus highly desirable to find a method which enables using at least some of these measurements for data analysis.

The key to such a correction lies in the fact that in many cases, only individual detector pixels are affected by radiation in the SAA. If they can be identified by their larger than normal signal, they can be flagged and excluded from the analysis. The remaining unaffected points in the spectrum can then be used for a standard retrieval with nearly the same quality as for spectra not affected by the SAA. Depending on the number of spectral points in a retrieval window, also more than one value can be excluded without compromising the retrieval quality too much.

1. SPIKE REMOVAL APPROACHES

In this study, two different approaches to spike correction have been evaluated, one based on work performed for OMI (Kleipool, 2005) which uses comparisons of consecutive measurements to identify spectral points with suspiciously large changes and one based on analysis of the DOAS fitting residuals as proposed by Richter et al., (2011).

In the following, the two approaches will be briefly presented. Then their application to GOME-2 data will be described and the optimisation of input parameters will be discussed. This will be followed by an investigation of the effects of application of spike correction on real data. Finally, a summary and conclusions will be given.

1.1 Spike Correction on Lv1 Data

An approach to spike identification and removal applied in the lv0 to lv1 processing was already developed for the OMI instrument (Kleipool, 2005), resulting in good suppression of SAA effects in data from that instrument. In this algorithm, outliers are identified in the spectral data by analysing the ratio of subsequent measurements in space and time. This approach is particularly well suited for the 2-dimensional CCD used in OMI but has here been adapted for GOME-2. As the correction is applied to lv1 data, it has the potential to improve all lv2 products including those which are not part of the operational processor.

1.2 Spike Correction in the DOAS Fit

In a recent paper, Richter et al. (2011) proposed an approach to correct for the spikes within the DOAS retrievals and demonstrated that a significant reduction in the scatter of NO_2 values can be achieved. The basic idea of this method is to run the DOAS retrieval on the data and then to scan the residual spectra of the fit for spectral points which are outliers in the sense of having a value much larger than the RMS of the total residual (excluding that point). For cases where such outliers are identified, they are flagged as bad spectral points and the fit is repeated on the remaining points. While Richter et al. (2011) tested the method for NO_2 only, it has also proven to work successfully for other trace gases such as SO_2, BrO, and HCHO.

1.3 Comparison of approaches

The two approaches have different advantages and disadvantages that have to be considered when deciding which of the two methods to use in GOME-2 operational processing.

The main advantages of the correction on lv1 data are

- On a conceptual level, this is the right approach to flagging of lv1 data
- Can be easily integrated into lv0 => lv1 processing or as pre-processing step of the lv2 processing
- Has only to be performed once and should then improve results for all lv2 products
- No implementation change in lv2 processors needed

The main disadvantages of the correction on lv1 data are

- Two parameters which need to be determined

- Some real changes in the spectra (Ring effect, wavelength shifts) might be interpreted as spikes
- Sensitivity is limited by atmospheric effects which are not removed from the data before the algorithm for correction is applied

The main advantages of the correction in the DOAS fit are

- Simple implementation in the DOAS retrieval
- Only one parameter needed which turns out to be a constant
- Very good sensitivity as all atmospheric effects are considered prior to correction

The main disadvantages are

- Significant increase in lv2 processing time
- Changes in all lv2 codes are necessary
- Potentially a conceptual problem arises as optimisation of chisquare by removing "bad" points could also hide real atmospheric effects or retrieval errors

2. APPLICATION: SPIKE CORRECTION ON LV1 DATA

2.1 Algorithm

The approach used for spike correction on lv1 data is to exploit the fact that spectra taken shortly after each other should be quite similar with respect to changes at short wavelength intervals, and that spikes are transient signals which affect individual spectra only. Any high frequency differences between adjacent spectra are either noise or – if larger than a certain threshold – indication for a spike.

The original algorithm (Kleipool, 2005) was developed for OMI where both the spatial and the spectral direction on the CCD can be exploited for identification of spikes. Also, the small spatial area and small full well capacity of CCD detector pixels allows easy detection of spikes.

Here, a simplified algorithm has been tested which is adapted to the GOME-2 situation.

Each spectrum is divided by the previous one to determine the change of the measurements. The ratio is then high pass filtered using a median filter to isolate high frequency structures. Spectral points having a high pass filtered ratio larger than a certain threshold are then flagged as spikes:

$$\left(\frac{\frac{y_n(\lambda)}{y_{n-1}(\lambda)}}{\overline{\frac{y_n(\lambda)}{y_{n-1}(\lambda)}}_{W_m}} \right) > \Theta$$

Here, the bar stands for the median with window W_m and $y_n(\lambda)$ is the spectrum n at wavelength λ. This algorithm has two parameters, the window of the median filter W_m and the threshold of the spike identification Θ. In Kleipool (2005), some values are given for the size of the median window depending on OMI channel while the spike threshold is linked to the estimated uncertainty of the individual spectral measurement point. Here both, the optimum width of the median window and the spike threshold are determined empirically (see Section 2.2). An overview on the algorithm flow is given in Figure 2.

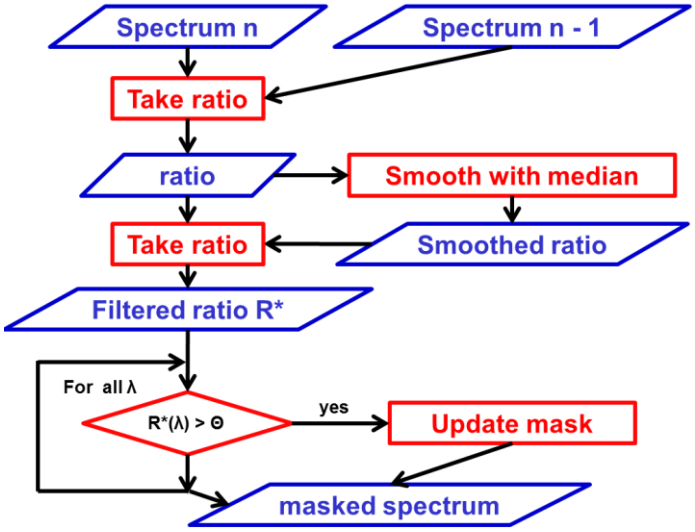

Figure 2: Schematic of the spike correction on lv1 data

2.2 Selection of Spike Threshold for NO_2

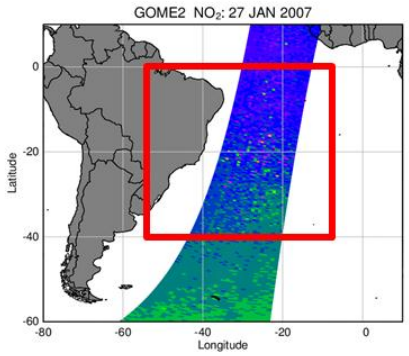

Figure 3: Orbit and region used for evaluating the use of different Spike correction threshold values

In order to investigate the effect of different choices for the parameters W_m and Θ, the RMS of the NO_2 vertical column for retrievals performed on lv1 data treated with spike correction applying various values for the two parameters were analysed for a single orbit (11774) in the region affected by the SAA (see Figure 3).

The range of values to be tested was set to 2 to 40 for the median window W_m and to 2 – 7 for the threshold Θ. The threshold is here determined as factor by which a point in the high pass filtered ratio R^* must be larger than the average deviation from 1 within the 5 * W_m values around the current point. As shown in Figure 4, the largest improvement in NO_2 RMS is achieved for the smallest threshold and for values for W_m around 20. Overall, a RMS reduction of up to 35% is achieved for this choice of parameters, and while the threshold should not exceed 2, choice of the median window is not critical.

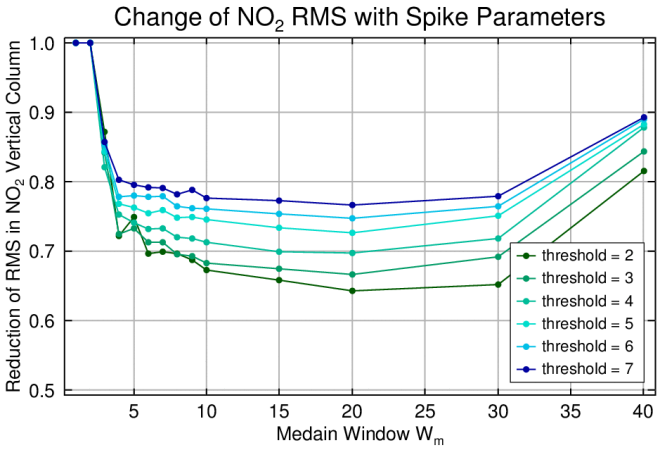

Figure 4. Improvement of RMS of NO_2 vertical column for different choices of the parameters Θ and W_m in the spike correction algorithm

3. APPLICATION: SPIKE CORRECTION IN THE DOAS FIT

3.1 Algorithm

In the approach using the fit residual for spike identification, the standard DOAS retrieval is performed on the uncorrected data. One of the outputs of the DOAS retrieval is the squared difference between model and measurement for each spectral point from which the RMS of the fit (the residual) is computed.

The algorithm now identifies those spectral points for which the difference between measurement y and model y_0 is larger than the average difference by a factor Θ, the Spike Threshold. More specifically, all spectral points λ_j for which

$$\left(y(\lambda_j) - y_0(\lambda_j)\right)^2 > \Theta * \sum_i \frac{\left(y(\lambda_i) - y_0(\lambda_i)\right)^2}{N - N_{spikes} - 1}$$

are flagged as spikes. Here, the sum on the right hand side of the equation is over all points not identified as spikes. In practice, this step therefore needs to be performed iteratively until no additional spikes are found.

Then the DOAS retrieval is repeated but taking into account only those points which are not flagged as spikes. A schematic description of the algorithm is shown in Figure 5.

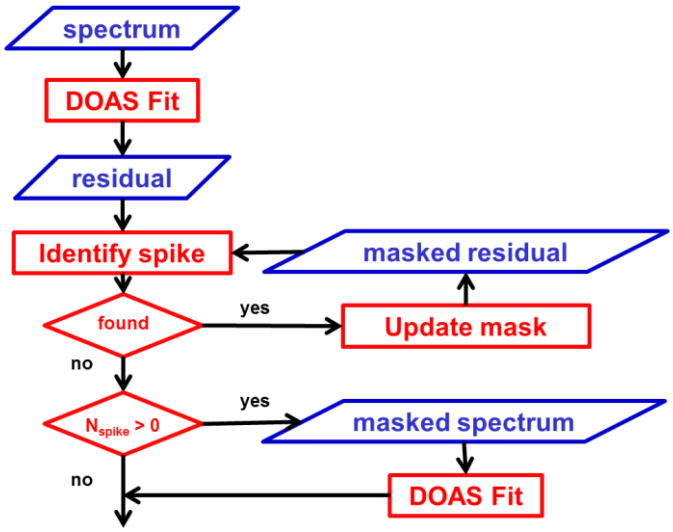

Figure 5: Flow chart of the spike removal in the DOAS fit. A spike mask is successively created from the residual of the first fit and finally applied to the spectrum before running the second fit (if necessary).

3.2 Selection of Spike Threshold for NO_2

In Figure 6, the effect of spike correction on NO_2 slant columns is illustrated for a part of one orbit crossing the SAA region. As can be seen from the red curve, the retrieval without spike correction displays large scatter including a number of points with negative values. The number of outliers and their magnitude can be reduced by application of the spike removal described above. Different

values for Θ were used leading to varying levels of improvement, the best results being obtained for Θ = 10 according to visual inspection.

A more quantitative assessment of different Θ values can be achieved by computing the RMS of the NO_2 values for a series of Θs. The results are shown in Figure 7 for three orbits, one from 2007, one from 2009, and one from 2012. In all cases, improvements are already found for very large Θ values, but an optimum in the RMS is obtained at Θ = 5..10. For even smaller Θ values the results deteriorate, probably because too many spectral points are removed making the retrieval unstable. As the minimum for the RMS is relatively broad, a conservative threshold of Θ = 10 appears to be the best choice.

The GOME-2 on Metop-A instrument suffers from relatively strong throughput degradation (Dikty et al., 2011). It is therefore important to check, if the best threshold value changes over the life time of the instrument. As shown in Figure 7, this does not seem to be the case, simplifying implementation of this approach.

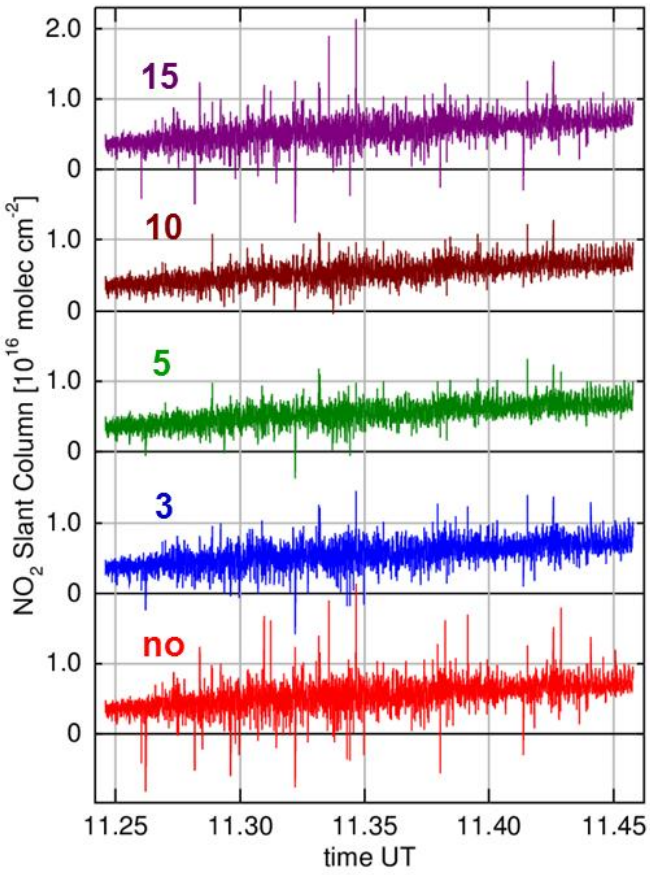

Figure 6: NO_2 slant columns (425 – 450 nm fitting window) for the part of GOME-2 orbit 11774 passing through the SAA retrieved without spike correction (red) and with varying levels of the spike threshold (3, 5, 10, 15).

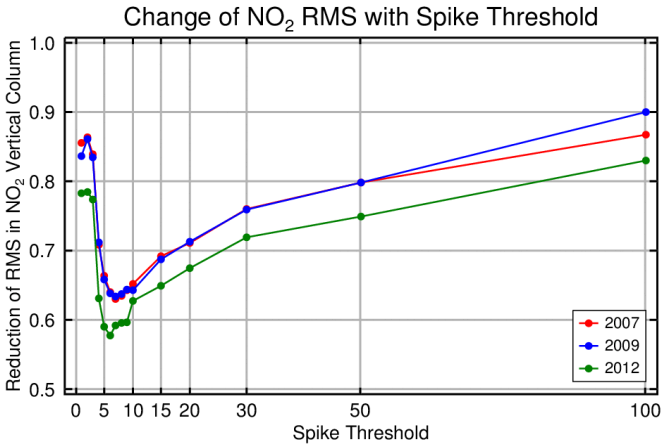

Figure 7: Reduction in RMS of NO_2 vertical columns from the fitting window 425 – 450 nm in the test region for different choices of the Spike Threshold value. A minimum is found for values between 5 and 10 independently of year of measurement.

3.3 Selection of Spike Threshold for other trace gases

The same approach as taken for NO_2 in Section 3.2 was also taken for other trace gases. In principle, one should expect to see differences in the behaviour of the retrievals as a function of Spike Threshold depending on the fitting window used, the absorption strength of the species of interest and the radiance intensity. However, tests for BrO and SO_2 showed surprisingly similar results as the analysis for NO_2 with $\Theta = 10$ being a good choice for these retrievals as well. This is probably explained by the fact that the best value of Θ is determined not so much by the details of the DOAS fit but more by the characteristics of the number, intensity and frequency distribution of the spikes.

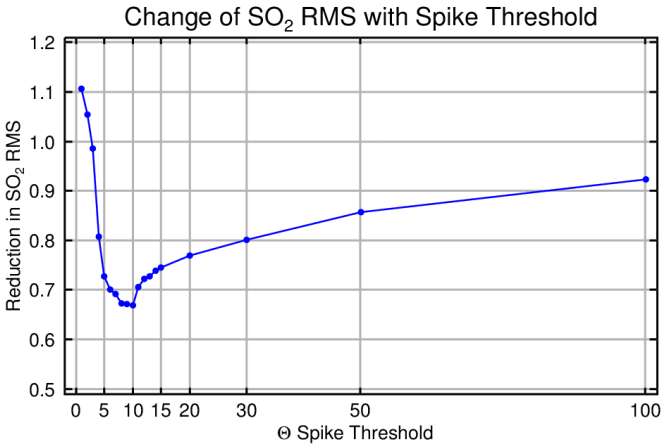

Figure 8: Reduction in RMS of SO_2 vertical columns from the 312.5 – 327 nm fitting window in the test region for different choices of the Spike Threshold value.

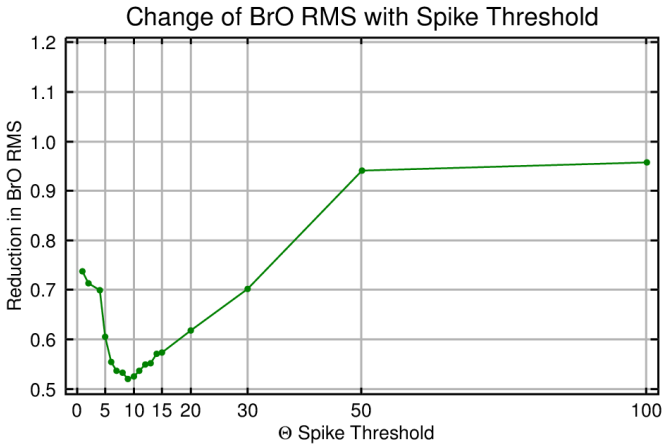

Figure 9: Reduction in RMS of BrO vertical columns from the 336 – 347 nm fitting window in the test region for different choices of the Spike Threshold value.

While these tests are clearly not exhaustive, the results all indicate that a universal selection of $\Theta = 10$ should result in significant improvements in the slant and vertical columns of all minor DOAS absorbers retrieved from GOME-2 measurements.

4. EVALUATION OF SPIKE CORRECTION

In the following, the effects of spike removal are discussed in detail. Nearly all of the discussion is based on results from the DOAS implementation. This choice was made for practical reasons as a larger data set (and more experience) with this correction was already available at IUP Bremen. However, it is to be expected that the results for the correction based on lv1 correction are very similar.

4.1 Spatial Distribution of Spikes removed

Depending on the spike removal threshold selected, a varying number of spectral points is removed from each spectrum. Ideally, all spectra should remain unchanged with the exception of those affected by the SAA or other disturbances. However, depending on the choice of spike threshold, values which through random noise have a larger deviation from the fit model will also be excluded. While this could be minimized by selection of a conservative threshold, a compromise needs to be found between effectiveness of the correction and removal of random points.

It therefore is important to evaluate the effect of the spike removal not only in the SAA but on a global scale. In Figure 10, the average number of spikes found and removed in the NO_2 retrieval (large fitting window 425 – 497 nm) is shown. As can be seen, most spikes are removed in the SAA region as expected, and this region does not only extend over most of South America but includes even parts of South Africa. In all other regions, between 1 and 2 spectral points are removed on average from each measurement with somewhat higher values at large SZA.

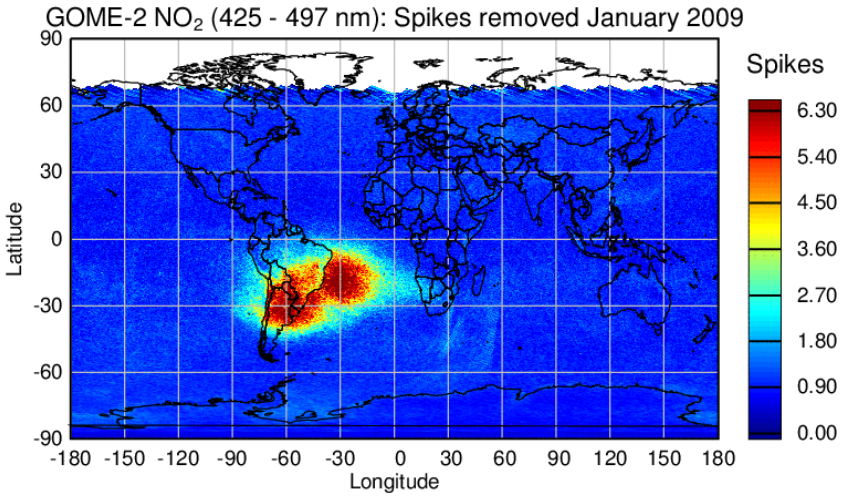

Figure 10: Number of spikes removed on average from each spectrum in GOME-2 NO_2 fits (425 – 497 nm) for January 2009. Only forward scans with SZA < 85° are included here as appropriate for a tropospheric NO_2 product.

Closer inspection of Figure 10 shows an area with higher values south east of Africa. This signature is the result of a large number of spikes removed in two orbits on January 26 as shown in Figure 11. Without spike correction, this area has large chisquare and unrealistic NO_2 columns on that day, and similar signatures are apparent in SCIAMACHY observations. While the reason for this disturbance is not known at this point, it can be concluded that something resulted in increased noise levels of satellite observations in that region on this day and that the spike correction scheme could strongly reduce the effect of this disturbance on the lv2 products.

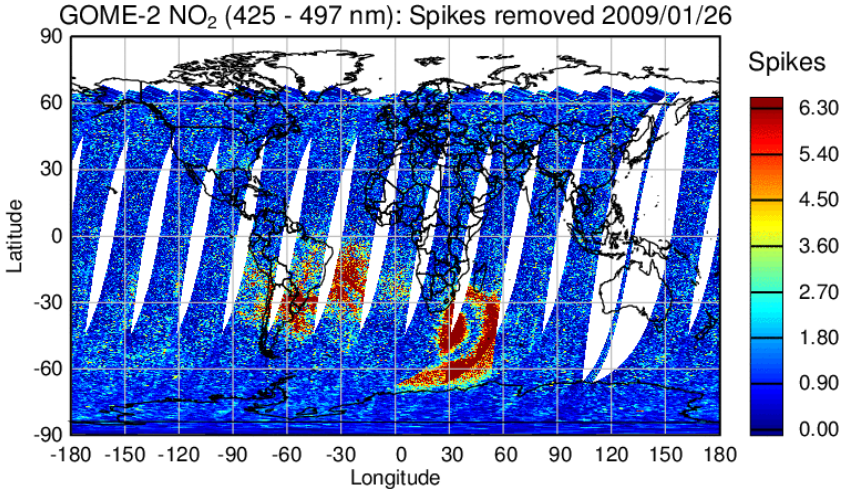

Figure 11: Number of spikes removed from each spectrum in GOME-2 NO_2 fits (425 – 497 nm) on January 26, 2009. See text for details.

Apart from this very unusual event, there are frequently individual spikes removed from spectra taken well outside the SAA. This is illustrated in Figure 12 for an orbit from January 24, 2009

showing how the spike correction can bring individual outliers into line by flagging detector pixels with erroneous values.

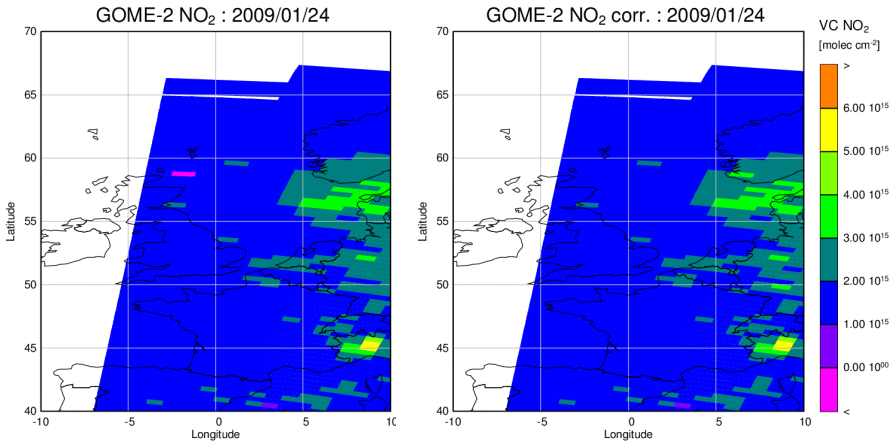

Figure 12: Example for removal of an outlier south of the Shetland Islands, an area not affected by the SAA. Shown are the NO_2 vertical columns from the small fitting window (425 – 450 nm) without (left) and with (right) spike correction.

4.2 Improvement in NO_2 RMS

In order to quantify the improvement achieved by using the spike correction, NO_2 retrievals should ideally be compared to independent validation data. However, such data is not available on a global scale, and therefore a pragmatic approach was used in which the RMS of NO_2 columns in a 1° x 1° grid cell is evaluated and the change in RMS between the analysis with and without spike correction is computed. Here the assumption is that any reduction in NO_2 RMS is indicative of an improvement in the retrieval.

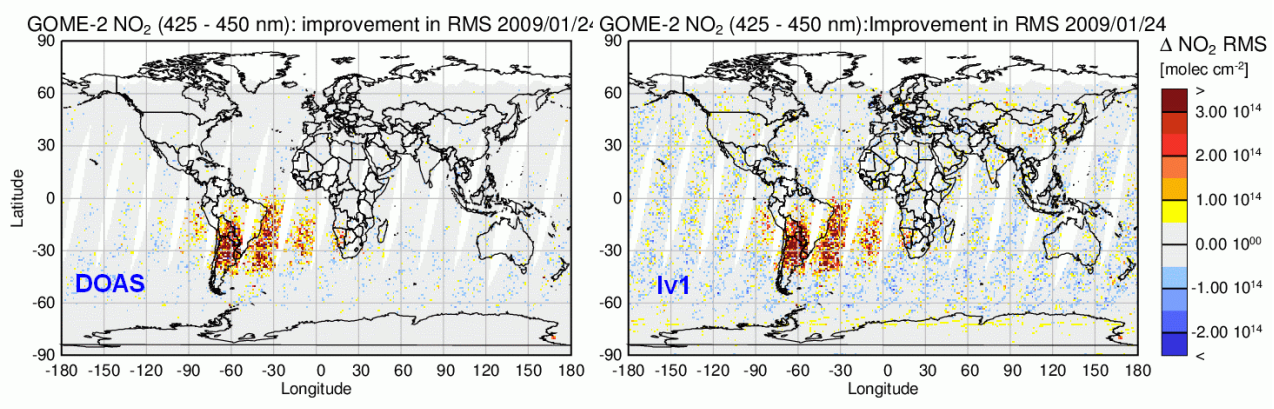

Figure 13: Reduction in NO_2 RMS per 1° x 1° grid cell for January 24, 2009. Left using DOAS spike correction with a threshold of 10, right using lv1 spike correction with threshold 2 and median window 20.

As shown in Figure 13 for one day of NO_2 retrievals, clear reductions in NO_2 RMS are achieved in the SAA region while elsewhere, the RMS remains basically unchanged as expected. The same is true even for monthly averages (see Figure 14), illustrating the improvement obtained through spike correction even in a data set averaged over 30 days.

Also shown in Figure 13 is the improvement when using lv1 spike correction. This yields very similar improvements but somewhat more noise in the regions outside the SAA. This is the result of the low threshold value which is needed to get sufficient improvement in the SAA region but also removes many values elsewhere reducing fitting quality. This aspect needs to be further investigated.

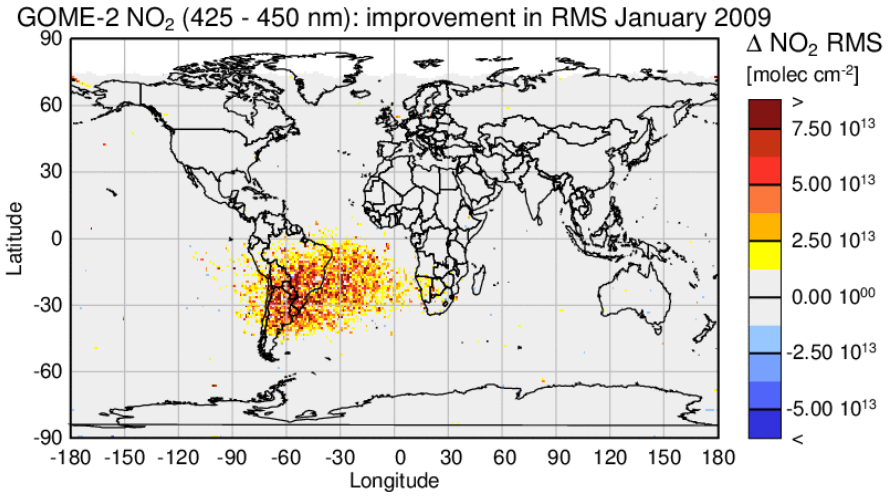

Figure 14: As Figure 13 but for the average of January 2009

Even larger improvements in NO_2 RMS can be achieved by combining a larger fitting window (more spectral information) with the spike removal algorithm (Richter et al., 2011). In particular the combination of both approaches proves to be useful as in a larger fitting window, the probability for having enough information for a stable NO_2 retrieval after removal of spectral points affected by spikes is larger. The additional improvement which can be achieved is illustrated in Figure 15 where the NO_2 RMS is shown for monthly averages of January 2009 data. Large RMS is apparent in regions with anthropogenic emissions (spatial gradients within the 1°x1° gridding boxes) and in the region affected by the SAA. As can be seen, combing a large fitting window with spike correction nearly removes the problem in monthly averages.

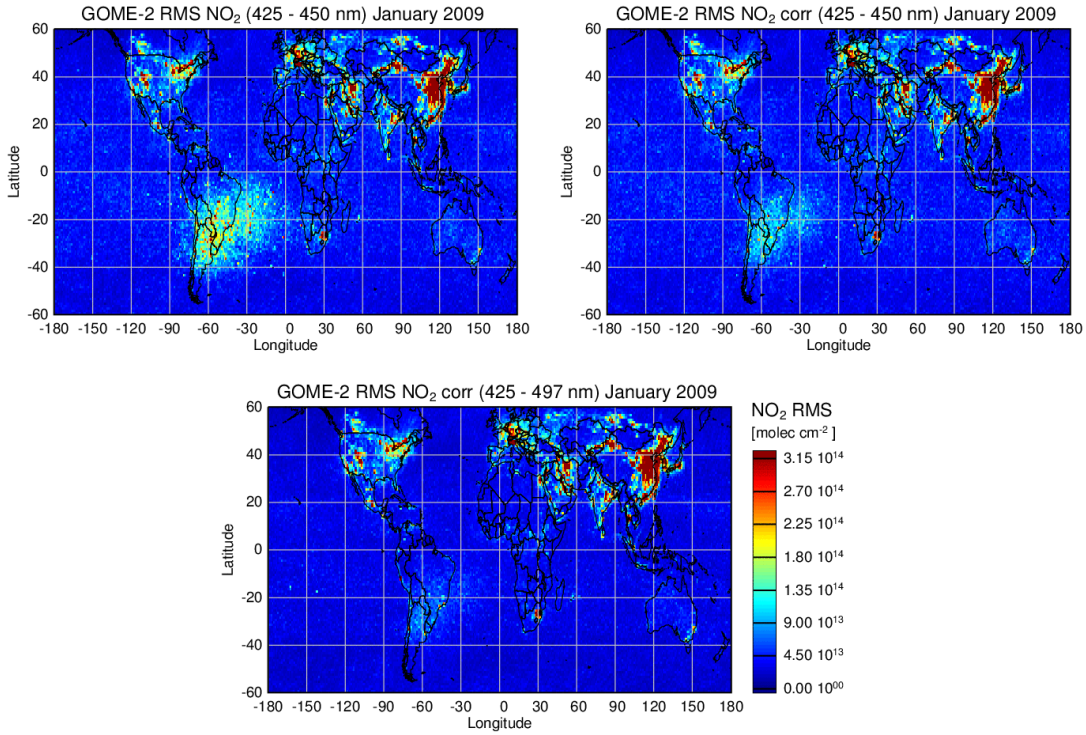

Figure 15: Spatial RMS of the vertical NO_2 columns for January 2009 on 1° x 1° bins for the small fitting window without correction (top left), with spike correction (top right) and for the large fitting window with spike correction (bottom)

4.3 Effect on NO_2 values

In addition to the reduction in scatter as documented in Section 0, any change in absolute NO_2 values needs also to be evaluated. This is shown for one example orbit through the SAA in Figure 16, where the difference between the NO_2 slant columns with and without spike correction is shown. On average, the differences outside the SAA are small ($< 5x10^{13}$ molec cm^{-2}) with the exception of large SZA values where NO_2 slant column differences can reach up to $2x10^{14}$ molec cm^{-2}. Considering typical air mass factors of > 10 at large SZA, the differences are on the order of one per cent of the expected NO_2 vertical columns. However, as shown by the error bars, individual fits can change by more than that leading to deviations of several per cent. While these effects might need some more attention, they are considered to be small enough to be acceptable.

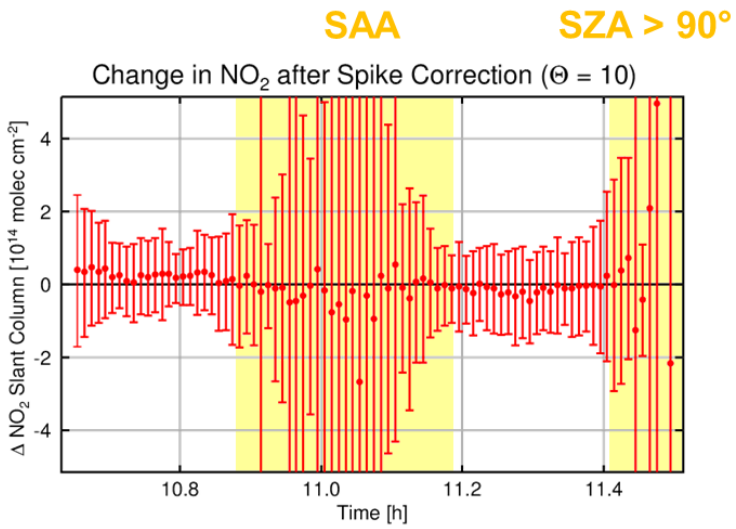

Figure 16: Difference in NO_2 slant column with and without spike correction for the orbit shown in Figure 3. Points are average values; error bars indicate 1 sigma standard deviation.

5. SUMMARY AND CONCLUSIONS

Two different approaches to spike correction in GOME-2 data have been described and investigated. One method is based on evaluating changes in consecutive lv1 radiances and identifying unrealistically large changes while the second algorithm is integrated in the DOAS retrieval and removes spectral points having a larger than expected residual.

Both methods have been demonstrated to improve the quality of GOME-2 NO_2 lv2 data. The DOAS implementation provides slightly better results, but further fine tuning of the parameters could probably bring the two methods to the same level. There is indication that the lv1 based approach decreases fitting quality outside the SAA region by removing too many good points if using thresholds appropriate for the SAA. If more conservative values are chosen, this effect is suppressed but at the same time, the spike removal in the SAA is less efficient. The final choice of algorithm should be based on implementation considerations.

For both algorithms, different values for the parameters needed were evaluated. For the DOAS spike removal, a threshold value of $\Theta = 10$ appears to be the best choice independently of trace gas and year of GOME-2 operation. For the lv1 based approach, the median window should be selected as $W_m = 20$ and a relative threshold of $\Theta = 2$ should be selected. These values were derived using only one orbit of NO_2 data and need to be confirmed.

Overall, the scatter of NO_2 values is largely reduced in the SAA affected region, and some outliers in other areas are also removed. The absolute columns of NO_2 are changed only slightly with somewhat larger changes at SZA > 90°, indicating that no significant change in product has to be expected outside the SAA area.

Further improvement in the scatter of the NO_2 product was demonstrated if the spike correction is combined with the use of a larger fitting window.

6. REFERENCES

Dikty, S, Richter, A., Weber, M., Noel, S., Wittrock, F. Bovensmann, H., Munro, R., Lang, R., Burrows, J.P., GOME-2 optical degradation as seen in level 2 data time series (2007 - 2010; BrO, NO2, HCHO, H2O, and O3), *EGU General Assembly, Vienna, Austria,* April 2011

Kleipool, Q.L., Transient signal flagging algorithm definition for radiance data**,** TN-OMIE-KNMI-717, 2005, available at http://www.atmos-meas-tech-discuss.net/4/C143/2011/amtd-4-C143-2011-supplement.pdf

Richter, A., Begoin, M., Hilboll, A., and Burrows, J. P.: An improved NO2 retrieval for the GOME-2 satellite instrument, *Atmos. Meas. Tech.* , **4**, 1147-1159, doi:10.5194/amt-4-1147-2011, 2011